Design and Analysis of Trench-Assisted Low-Bending-Loss Large-Mode-Field-Area Multi-Core Fiber with an Air Hole

Renjie Jia [1,2], Yudong Lian [1,2,3,*], Yulei Wang [1,2] and Zhiwei Lu [1,2]

1 Center for Advanced Laser Technology, Hebei University of Technology, Tianjin 300401, China; 183975@stu.hebut.edu.cn (R.J.); wyl@hebut.edu.cn (Y.W.); zhiweilv@hebut.edu.cn (Z.L.)
2 Hebei Key Laboratory of Advanced Laser Technology and Equipment, Tianjin 300401, China
3 Tianjin Key Laboratory of Electronic Materials and Devices, Tianjin 300401, China
* Correspondence: ydlian@hebut.edu.cn

Abstract: In this paper, a trench-assisted low-bending-loss large-mode-field-area multi-core fiber with air hole is proposed, which can achieve dual-mode transmission. The influence of structural parameters on fiber performance is analyzed systematically, and the structure of the trench, with a lower refractive index than the cladding, is also analyzed and optimized. By adjusting the structural parameters, the effective mode field area of the fundamental mode can reach 2003.24 um^2 at 1550 nm, and when the bending radius is 1 cm, the bending loss is 2.57×10^{-3} dB/m. The practical implementation of the proposed fiber is feasible using existing fabrication technology and is applicable to the transmission of large-capacity optical communication systems and high-power lasers.

1. Introduction

The advent of the "Internet +" era and the 5G era have put forward higher requirements for the high speed and high bandwidth of optical communication networks. Ultra-high-speed, large-capacity, and ultra-long-distance transmission has become the future trend. The conventional single-mode single-core fiber (SM-SCF) is gradually approaching its 100 Tb/s transmission limit due to the limitation of the nonlinear effect [1]. The rapid development of communication technologies such as wavelength division multiplexing (WDM) and polarization multiplexing (PDM) enables mode division multiplexing (MDM) based on few-mode fibers to be used to increase channel transmission capacity [2]. Increasing the mode field area can reduce the nonlinear effect of the fiber, but it will also increase the number of transmittable modes in the fiber and bring about bending loss. Therefore, low-bending loss and large-mode area few-mode fibers have important research significance in high-power optical communication devices [3].

In recent years, fiber lasers have developed rapidly. In order to overcome the limitation of fiber laser power improvements such as the fiber nonlinear effect and fiber damage, the method of increasing the mode field area can be used to overcome the nonlinear effect. The strong coupling multi-core fiber (MCF) increases the mode field area (MFA) of the fiber by introducing the lateral coupling of the core, thereby reducing the nonlinear effect. Therefore, it is often used in fiber lasers and amplifiers [4]. But multi-core fibers have a higher bending loss [5]. However, the reduction of the bending loss (BL) is conducive to improving the stability and output efficiency of the fiber laser source [6,7]. Adding air holes and a trench in cladding can effectively reduce the bending loss.

Commonly used fiber structures for achieving a large mode field and low bending loss include: photonic crystal fiber, trench-assisted fiber, and multi-core fiber. The photonic crystal fiber has a large mode field area and good bending resistance. However, the structure is complex and asymmetric, and the technological level is high and welding is difficult. Usually, the effective mode field area can reach 794 um^2, and the bending

loss is 0.064 dB/m, when the bending radius is 15 cm [8]. The trench-assisted fiber has good bending resistance. However, due to process limitations, the width and depth of the submerged layer will be limited. The fiber can not only support ultra-low bending loss (0.052 dB/turn when bending radius R = 5 mm), but also support an effective mode field area of up to 260 um^2 at a working wavelength of 1.55 um [9,10].

Multi-core optical fiber has the characteristics of a symmetrical structure distribution, simple design, flexible parameter adjustment, and large mode field area. However, large mode field multi-core optical fiber often has a higher bending loss. The fiber can generally transmit with a low bending loss (less than 1.0 dB/m when the bending radius R = 0.34 m), and the effective area is as high as 1331 um^2 [11–15].

There is a mutually restrictive relationship between the bending loss of the optical fiber and the mode field diameter (mode field area). The smaller the mode field diameter, the better the light can be confined, thus reducing the bending loss of the fiber. But if the mode field diameter of the fiber is too small, there will be serious nonlinear effects under high power conditions [16]. Therefore, the two must be considered comprehensively.

A trench-assisted low-bending-loss large-mode-field-area multi-core fiber (TA-LBL-LMFA MCF) with an air hole structure is proposed in this paper that can realize dual-mode transmission. The MFA of the fundamental mode of the fiber can reach 2003.24 um^2. When the bending radius is 1 cm, BL can be as low as 2.57×10^{-3} dB/m. Using the existing fabrication techniques, the practical implementation of the proposed fiber is feasible.

2. Optical Fiber Structure and Theoretical Analysis

The fiber structure is shown in Figure 1. The yellow part is the central core and the gray part is the silica cladding. The blue part is a trench with a lower refractive index (RI) than the cladding. This structure adds 10 cores (green part) to the traditional hexagonal 19-core optical fiber structure (pink part), removes the cores on both sides of the 19-core optical fiber, and adds air holes and a trench in the cladding. The green part, yellow part, and pink part constitute the core area.
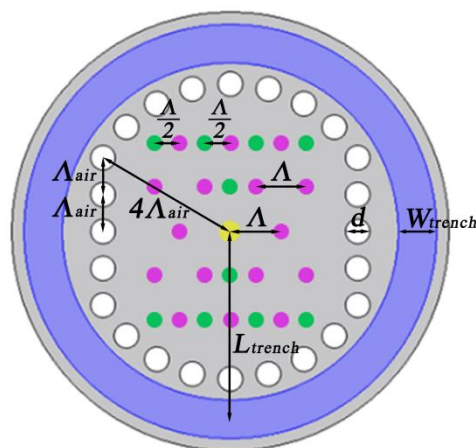

Figure 1. Schematic diagram of optical fiber cross section.

The diameter of the fiber cladding is d_{clad} = 125 um, the refractive index of the fiber cladding n_{clad} = 1.444, the refractive index of the air hole is the refractive index of air n_{air} = 1.000, the refractive index of the central core is n_{center}, and the refractive index of the other cores is n_{core}. The refractive index difference between the center core and the cladding is $\Delta n_{center} = n_{center} - n_{clad}$; $\Delta n = n_{core} - n_{clad}$ is the refractive index difference between the core and the cladding; Λ is the distance between the core and the core, Λ_{air} = 14 um is the spacing between the air holes, and d_{center} is the diameter of the central core. The diameter of the other cores is d, the diameter of the air hole is d_{air} = 7 um, and the refractive index of the trench is n_{trench}. $\Delta n_1 = n_{clad} - n_{trench}$, which is the refractive index difference between cladding and the trench; W_{trench} is the thickness of the trench layer, and L_{trench} is the distance between the trench layer and the central core. The

structural parameters are composed of seven parameters: Λ, d, Δn, d_{center}, Δn_{cneter}, W_{trench}, and L_{trench}.

This paper is mainly based on the finite element method (FEM) software to analyze the fiber structure [17].

The refractive index of the beam propagating in a specific mode changes with the wavelength and the geometric structure of the waveguide. This is called the effective refractive index n_{eff} of the mode. The conduction of specific mode in optical fiber needs to satisfy the conduction mode condition of the optical waveguide theory: $n_{eff} < n_{clad} < n_{core}$. Otherwise, the mode will be cut off and does not exist in the fiber. The effective refractive index n_{eff} calculation formula can be expressed as [18]:

$$n_{eff} = Re\left(\frac{\beta}{k_0}\right). \tag{1}$$

Among these figures, β is the propagation constant, the Re is the real part of the whole, the wave number in vacuum is $k_0 = 2\pi/\lambda$, and λ is the working wavelength.

The electromagnetic field of each mode along the cross section of the fiber is called the mode field. An optical fiber with a large mode field area can suppress the nonlinear effect in the optical fiber. The effective mode field area A_{eff} can be expressed as [19]:

$$A_{eff} = \frac{\int (EE^* dA)^2}{\int (EE^*)^2 dA} \tag{2}$$

where E represents the electric field of the mode, and E^* represents the conjugate complex number of the electric field of the mode.

When the fiber is bent in the positive direction of the x-axis, and the equivalent refractive index distribution of the fiber cross-section is [20]:

$$n(x,y) = n_0(x,y)\sqrt{1 + \frac{2x}{R_{eff}}}. \tag{3}$$

Among them, $n(x, y)$ is the equivalent refractive index of the fiber after bending, and $n_0(x, y)$ is the initial refractive index of the fiber. R is the bending radius of the optical fiber along the positive x-axis. When the elastic optical correction factor is introduced, the equivalent bending radius $R_{eff} = 1.28R$.

The calculation formula of fiber bending loss α can be expressed as [20]:

$$a = -\frac{20\pi}{ln10} IM(\beta) \approx -8.686\frac{2\pi}{\lambda} IM\left(n_{eff}\right) \tag{4}$$

where IM represents the imaginary part, and n_{eff} represents the effective refractive index of the fiber.

3. Analysis and Optimization of Optical Fiber Structure Parameters

The fiber structure can effectively destroy the circular symmetrical structure of the traditional 19-core optical fiber. It cuts off the higher-order modes (TE_{01}, TM_{01}), leaving two degenerate fundamental modes (HE_{11}) and second-order modes (HE_{21}), as shown in Figure 2. In addition, the 10 fiber cores increase the lateral coupling of the fiber, which significantly increases the mode field area of the fiber. The effective refractive index of the cladding is reduced by adding air holes and grooves in the cladding. As a result, the refractive index difference between the core and the cladding is increased, and the BL is significantly reduced.
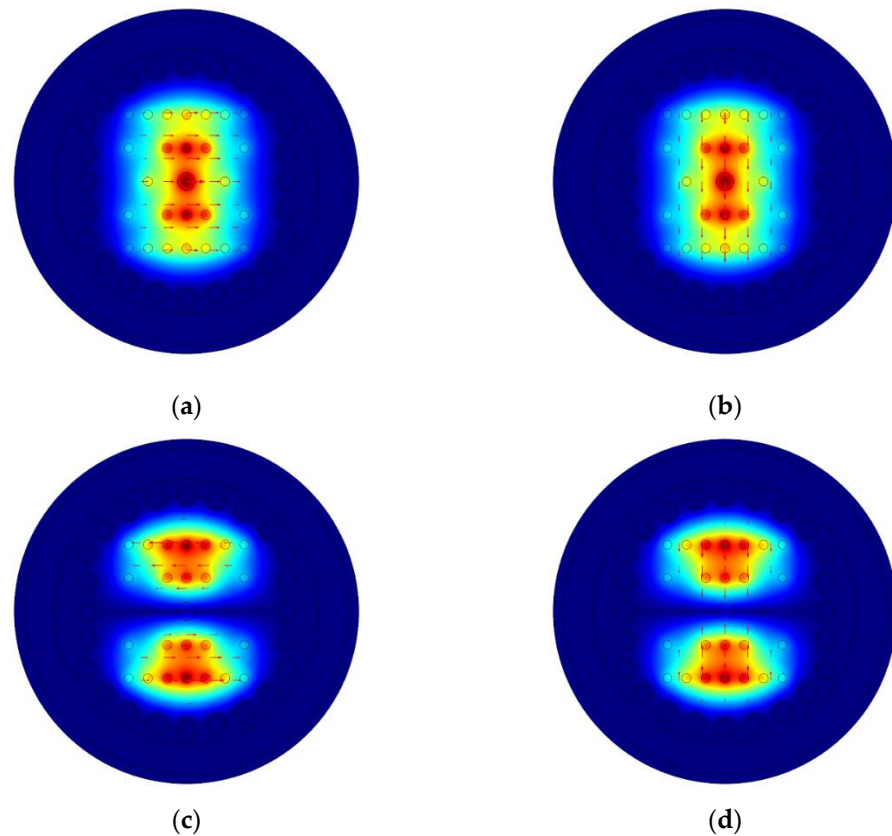
Figure 2. Optical fiber two-dimensional mode field and electric field distribution diagram: (**a**) HE_{11-x} mode; (**b**) HE_{11-y} mode; (**c**) HE_{21-x} mode; (**d**) HE_{21-y} mode.

3.1. Analysis of Three Structural Parameters Λ, d, and Δn

For this paper, we conducted research on the basis of strict dual-mode transmission. Λ, d, and Δn three structural parameters were analyzed. The working wavelength λ was set at 1550 nm, and the initial structure parameter was set as $\Lambda = 15$ um, $d = 3$ um, $\Delta n = 0.003$, $d_{center} = d$, $\Delta n_{center} = 0.003$, $W_{trench} = 5.5$ um, $L_{trench} = 52$ um, $\Delta n_1 = 0.004$.

The result of analyzing the influence of the structural parameter Λ on n_{eff} and A_{eff} is shown in Figure 3. To realize dual-mode transmission and cut high-order modes of optical fiber, its effective refractive index should be less than n_{clad}. Figure 3a shows that the transmission mode can be adjusted by modifying Λ. If dual-mode transmission is to be realized, Λ should be greater than or equal to 11.5 um. Figure 3b shows that as Λ goes from 10 um to 15 um, the A_{eff} of HE_{11} grows from 1451 um² to 2201 um² and then drops to 1996 um², and finally reaches the maximum value at 14.5 um; in addition, the A_{eff} of HE_{21} grows from 1219 um² to 1717 um². From the above discussion, it can be concluded that 14.5 um is the best choice for Λ.
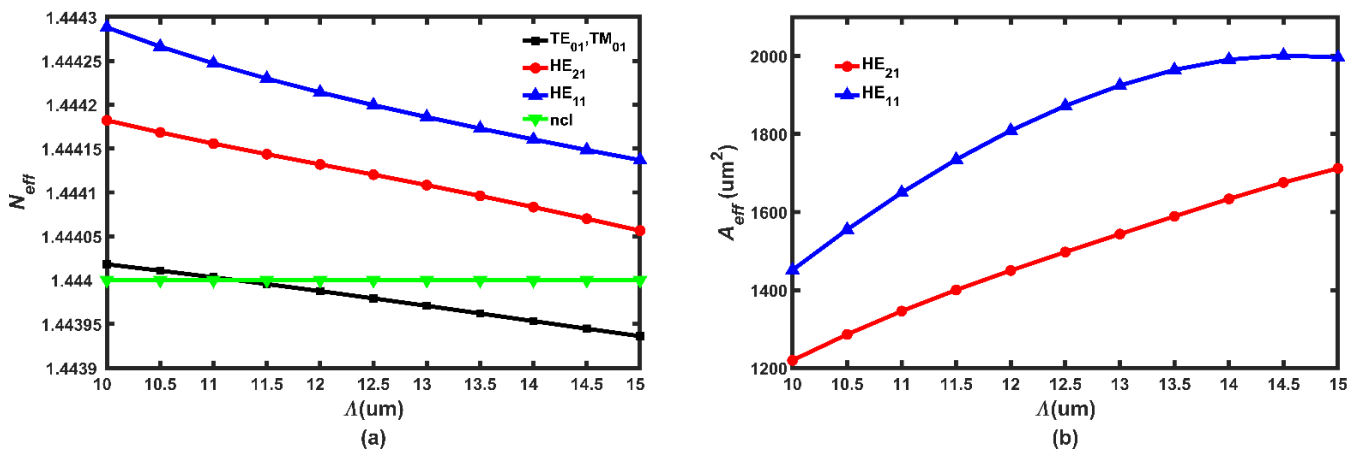
Figure 3. (**a**) The variation of N_{eff} with Λ for each mode; (**b**) The change of A_{eff} of HE_{11} and HE_{21} with Λ.

When Λ is 14.5 um, the results of analyzing the influence of structure parameter d on n_{eff} and A_{eff} are shown in Figure 4. Figure 4a shows that as d increases, the effective refractive index of each mode also increases. If d is less than or equal to 3.3 um, then the fiber realizes dual-mode transmission. It can be seen from Figure 4b that as d increases to 3.4 um, the A_{eff} of HE_{11} rises to the maximum value of 2032 um^2, and the A_{eff} of HE_{21} decreases from 1706 um^2 to 1616 um^2. However, due to the limitation of dual-mode transmission conditions, d is the most suitable to be 3.3 um. At this time, the A_{eff} of HE_{11} is 2029 um^2, and the A_{eff} of HE_{21} is 1632 um^2. Optical fiber can achieve dual-mode transmission, but also has a large A_{eff}.
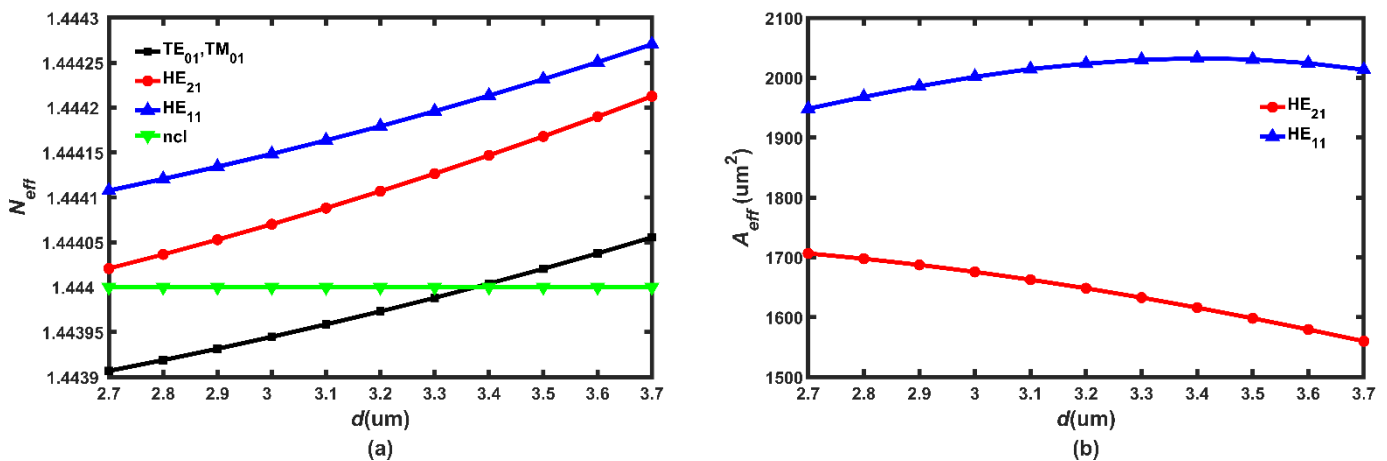

Figure 4. (**a**) Variation of N_{eff} with d for each mode; (**b**) the change of A_{eff} of HE_{11} and HE_{21} with d.

When d is 3.3 um, the effect of Δn on n_{eff} and A_{eff} is shown in Figure 5. Figure 5a shows that with the increase of Δn, the neff of TE_{01} and TM_{01} also increase. In order to ensure dual-mode transmission, Δn should be less than or equal to 0.00315. It can be seen from Figure 5b that the maximum A_{eff} of HE_{11} at 3.1 um is 2031 um^2 for Δn, and the A_{eff} of HE_{21} at this time is 1622 um^2. In order to ensure that the fundamental mode obtains a larger mode field area, Δn is selected as 0.003.

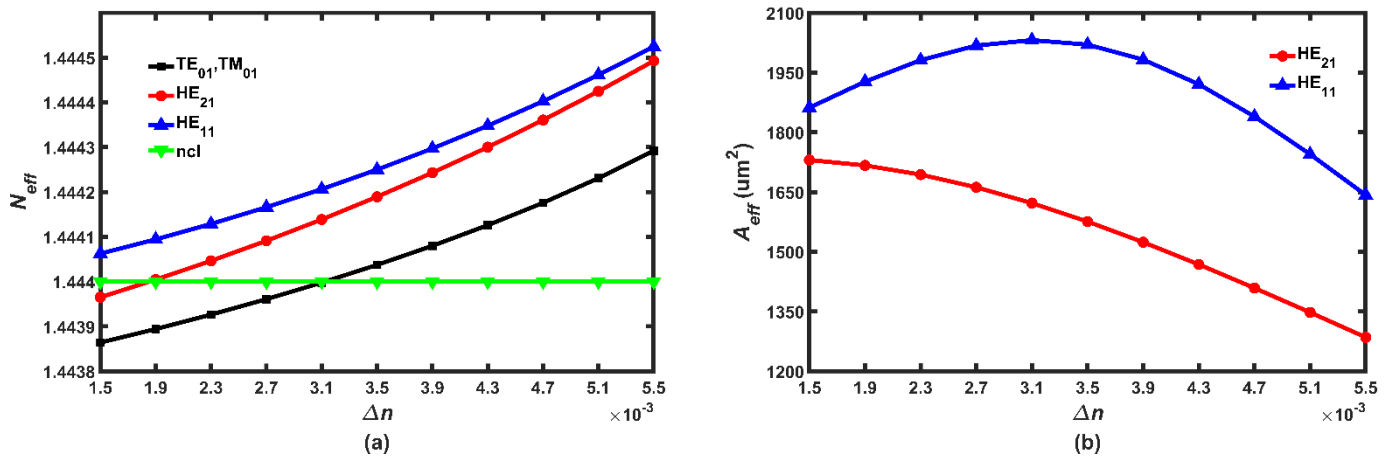**Figure 5.** (**a**) The n_{eff} of each mode varies with Δn; (**b**) the change of A_{eff} of HE$_{11}$ and HE$_{21}$ with Δn.

3.2. Analysis of Structural Parameters of Central Core

In order to enhance the core's ability to confine light, the central core diameter d_{center} is increased to reduce the central core refractive index Δn_{center}, thereby reducing the bending loss. This part analyzes the d_{center} and Δn_{center} structure parameters of the center core and initializes the center core structure parameters to $\Delta n_{center} = 0.001$ and $d_{center} = 3$ um.

Based on the optimization of the above structural parameters, the influence of d_{center} on n_{eff} and A_{eff} is studied, as shown in Figure 6. Figure 6a shows that the effective refractive index of the higher-order modes TE$_{01}$, TM$_{01}$ is around 1.444, intersecting with ncl at 7.2 um. To ensure dual-mode transmission, d_{center} should be less than 7.2 um. As shown in Figure 6b, HE$_{11}$ has the largest A_{eff} at 4.8 um in d_{center}, which is about 2039 um^2 and the A_{eff} of HE$_{21}$ has been stable around 1622 um^2, so 4.8 um is the best choice for d_{center}.

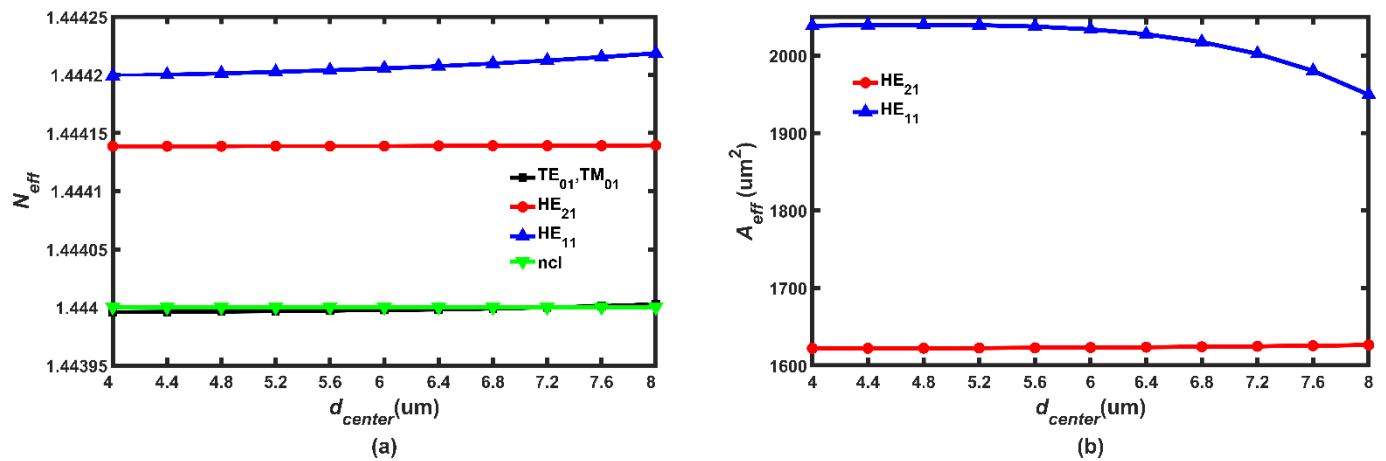**Figure 6.** (**a**) The N_{eff} of HE$_{11}$ and HE$_{21}$ varies with d_{center}; (**b**) The change of A_{eff} of HE$_{11}$ and HE$_{21}$ with d_{center}.

When the d_{center} is 4.8 um, the influence of Δn_{center} on n_{eff} and A_{eff} is shown in Figure 7. Figure 7a shows that TE$_{01}$, TM$_{01}$, and ncl intersect at 0.002. To ensure dual-mode transmission, Δn_{center} must be restricted within 0.002.
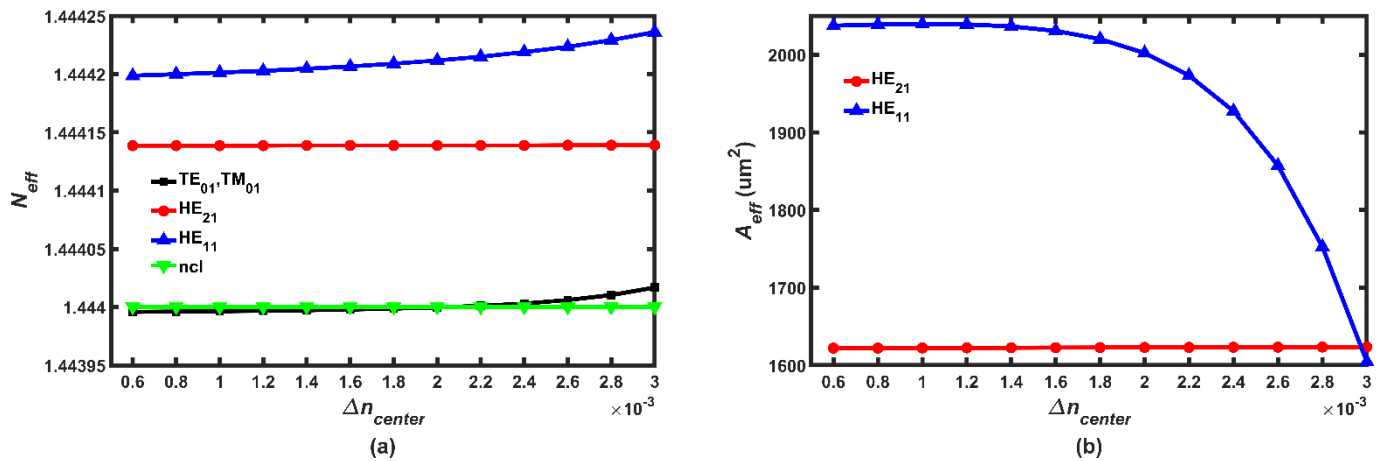
Figure 7. (**a**) The N_{eff} of HE$_{11}$ and HE$_{21}$ varies with Δn_{center}; (**b**) the change of A_{eff} of HE$_{11}$ and HE$_{21}$ with Δn_{center}.

The greater the refractive index of the central core of the optical fiber, the stronger its ability to confine light, but the mode field area will decrease. It can be seen from Figure 7b that when Δn_{center} exceeds 0.002, the A_{eff} of HE$_{11}$ decreases rapidly. The A_{eff} of HE$_{21}$ is stable at 1622 um^2, and the A_{eff} of HE$_{11}$ is 2002 um^2 at 0.002. Δn_{center} is selected as 0.002 as the best, which not only has a large mode field area, but also has a better ability to bind light.

4. Bending Characteristic Analysis

This part studies the effect of R on the A_{eff} and BL of HE$_{11}$ and HE$_{21}$ when the working wavelength is 1550 nm.

When the bending radius is 1.5 cm, the mode field and electric field will deviate from the core area to the direction of the trench as shown in Figure 8, resulting in a reduction in the mode field area and an increase in the bending loss. In order to prevent the electric field from deviating to the trench, a circle of air holes is added in the middle of the cladding. The air holes have a lower refractive index, which can effectively prevent the electric field from deviating to the trench. At the same time, it reduces the refractive index of the cladding and the bending loss is reduced.
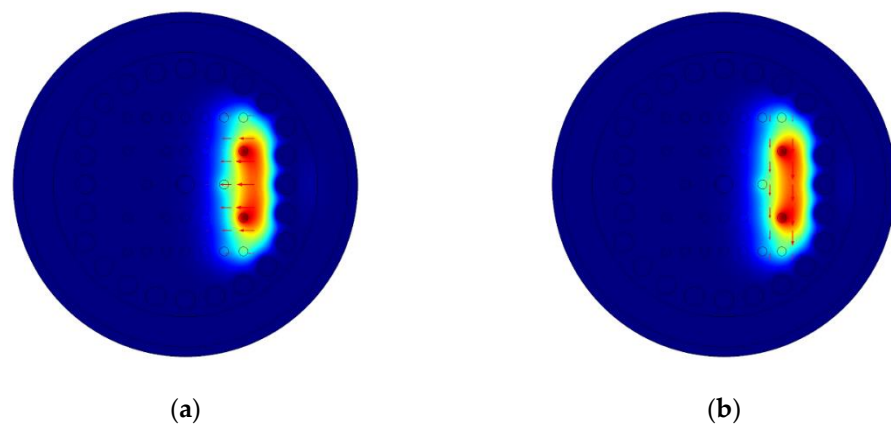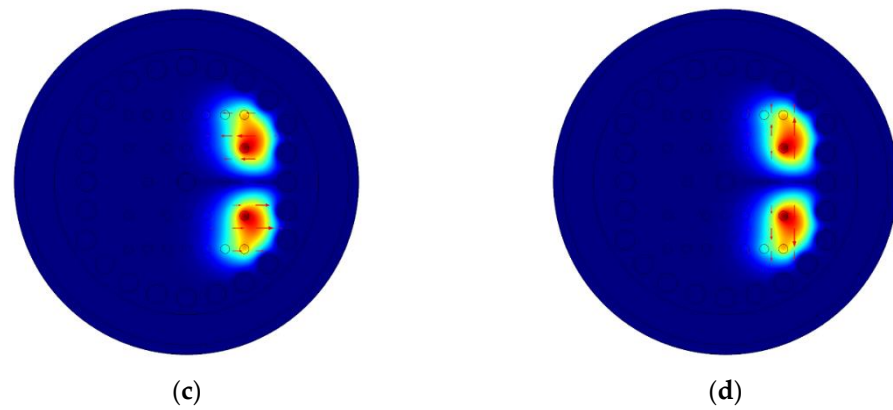

(**a**)

(**b**)

Figure 8. *Cont.*

Figure 8. The two-dimensional mode field and electric field distribution diagram of the fiber when the bending radius is 1.5 cm: (**a**) HE_{11-x} mode; (**b**) HE_{11-y} mode; (**c**) HE_{21-x} mode; (**d**) HE_{21-y} mode.

The two polarization states of a mode have the same changing trend and similar size, so the two polarization states are almost overlapped. Figure 9a shows that when R increases from 1 cm to 19 cm, the A_{eff} of HE_{11} and HE_{21} will also increase. After the bending radius is greater than 11 cm, the A_{eff} of HE_{11} and HE_{21} tends to be stable, around 2100 um^2 and 1600 um^2. Figure 9b shows that as R increases from 1 cm to 6 cm, the *BL* of HE_{11} and HE_{21} will also decrease. When the bending radius is 1.5 cm, the *BL* of the two modes is less than 10^{-3} dB/m. The fiber has very low bending loss. In the case of no bending, the A_{eff} of HE_{11} is 2003.24 um^2 and the A_{eff} of HE_{21} is 1686.71 um^2. Therefore, the optical fiber has good bending insensitivity.
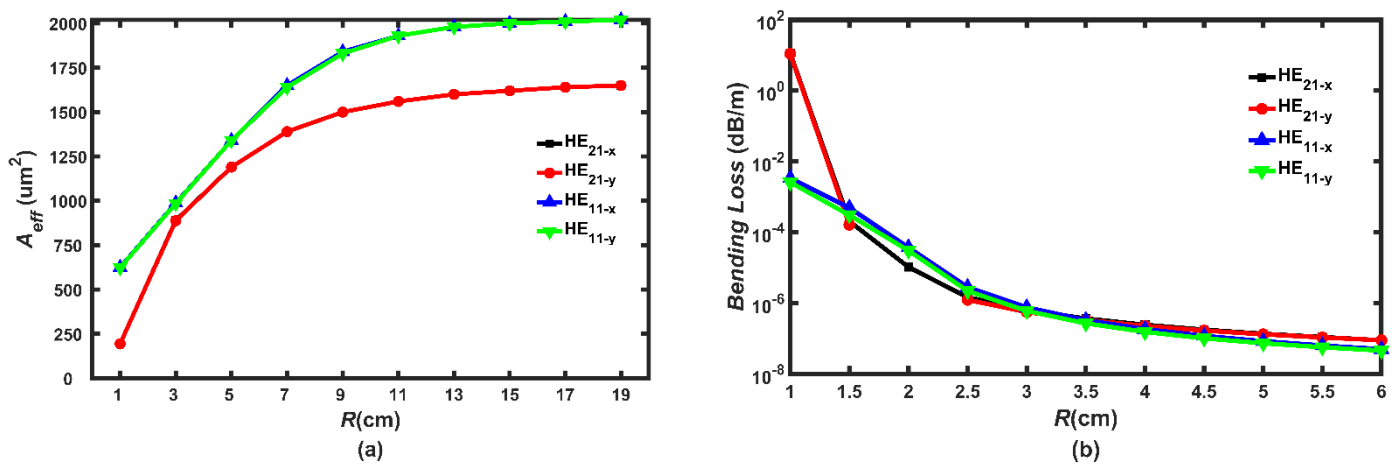
Figure 9. (**a**) The change of A_{eff} of HE_{11} and HE_{21} with R; (**b**) the *BL* of HE_{11} and HE_{21} changes with R.

Table 1 is a comparison table between this article and other recent work and literature.

Table 1. A comparison table with other recent work and literature.

Article	Description
[21]	Mode area of 2622 um^2 at a bend radius of 20 cm can be achieved. Bending loss can be reduced to about 0.092 dB/m at 1550 nm.
[17]	When the bending radius is 20 cm, the effective mode area of the fiber can reach 914 um^2 at 1.06 um, and loss ratio between lowest-HOMs and fundamental mode is larger than 100.
[22]	Mode field area of the fundamental mode can reach 1916.042 um^2 at 1550 nm., and when the bending radius is 1.4 cm, the bending loss is 2.96×10^{-3} dB/m.
This article	Mode field area of the fundamental mode can reach 2003.24 um^2, and when the bending radius is 1 cm, the bending loss is 2.57×10^{-3} dB/m at 1550 nm.

5. Structural Optimization of the Trench

Adding trench in the cladding can effectively reduce the bending loss of the optical fiber and improve the bending resistance of the optical fiber. However, the bending loss of the optical fiber and the mode field area are mutually restrictive, so the two parts must be taken into consideration at the same time in the design. In order to balance the relationship between the bending loss and the mode field area, this paper defines the performance factor *PI* [23] of the fiber, and the expression is:

$$PI = \frac{BL}{A_{eff}}. \tag{5}$$

PI is used to measure the trade-off between *BL* and A_{eff}. When A_{eff} increases and *BL* decreases, *PI* will decrease, and the comprehensive performance of the fiber will be better.

This section provides analysis and optimization of the L_{trench} and Δn_1 parameters of the trench. We used *PI* to evaluate the comprehensive performance of the optical fiber. W_{trench} has little effect on the A_{eff} of each mode, and the larger the thickness, the smaller the bending loss. Therefore, the larger the W_{trench}, the better the comprehensive performance of the fiber. However, W_{trench} is limited by the diameter of the cladding layer to a maximum of 5.5 um.

When the W_{trench} is 5.5 um, the influence of the L_{trench} on the A_{eff} and *PI* of the fiber under the condition of a 1.5 cm bending radius is shown in Figure 10. From Figure 10a, it can be seen that the A_{eff} of HE$_{11}$ drops rapidly at 53.9 um, and the A_{eff} of HE$_{21}$ slightly rises. When the L_{trench} exceeds 53.8 um, the trench will exceed the cladding and the structure will be disordered, resulting in a sudden change in the curve. It can be seen from Figure 10b that with the increase of L_{trench}, the *PI* of HE$_{11}$ first drops and then rises rapidly, with a minimum value at 53.8 um, while the *PI* of HE$_{21}$ is relatively stable. So, at 53.8 um, the fiber has the best comprehensive performance.
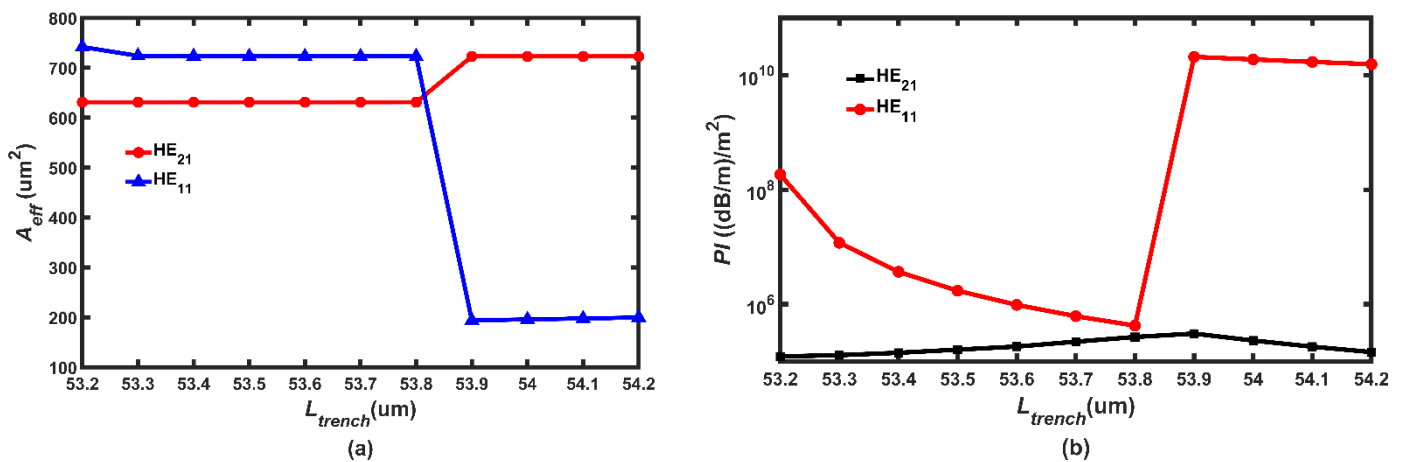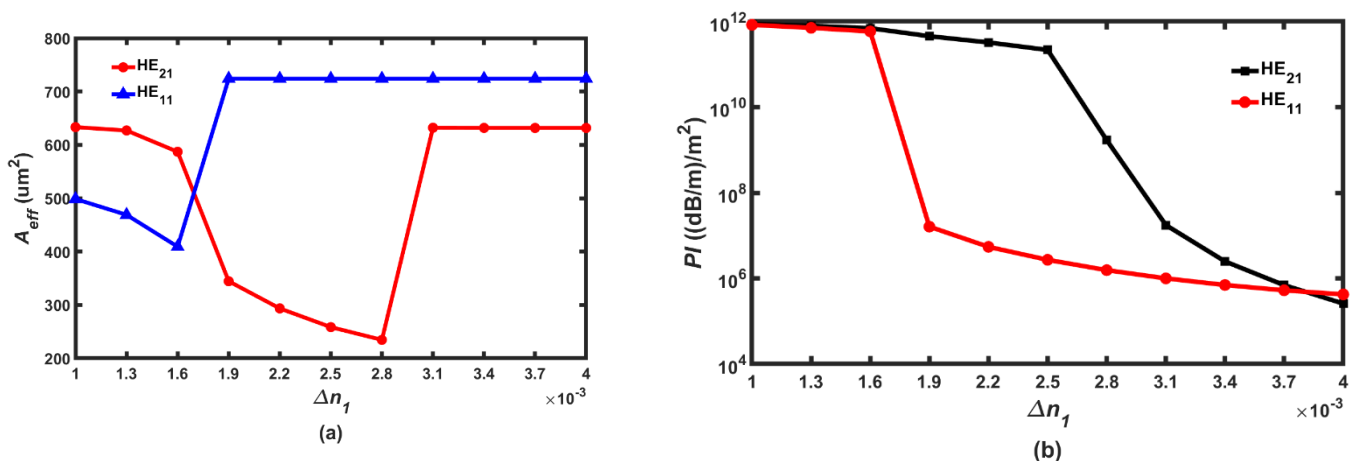

Figure 10. (**a**) The N_{eff} of HE$_{11}$ and HE$_{21}$ varies with L_{trench}; (**b**) The PI of HE$_{11}$ and HE$_{21}$ varies with L_{trench}.

When L_{trench} is 53.8 um, the influence of Δn_1 on N_{eff} and *PI* is shown in Figure 11. Figure 11a shows that with the increase of Δn_1, A_{eff} of the two modes firstly decreases, then increases, and finally stabilizes. In Figure 11b, the *PI* of the fiber decreases with the increase of Δn_1. This indicates that the larger the Δn_1, the better the comprehensive performance of the fiber. Due to the limitation of the manufacturing process, Δn_1 cannot be too large, and is usually set to 0.004.

Figure 11. (**a**) The A_{eff} of HE_{11} and HE_{21} varies with Δn_1; (**b**) the BL of HE_{11} and HE_{21} changes with Δn_1.

In summary, the final optimized parameters are as follows: $\Lambda = 14.5$ um, $d = 33$ um, $\Delta n = 0.0031$, $d_{center} = 4.8$ um, $\Delta n_{center} = 0.002$, $W_{trench} = 5.5$um, $L_{trench} = 53.8$ um, $\Delta n_1 = 0.004$.

6. Conclusions

A dual-mode TA-LBL-LMFA MCF with air hole structure is investigated in this paper. By removing the core on both sides of the traditional 19-core fiber, the fiber can destroy the circular symmetry structure of traditional 19-core fiber and cut off the high-order modes TE_{01} and TM_{01} with circular symmetry. Adding a circle of air holes at the periphery of the core area can confine the mode field in the core area effectively. Also, adding a trench that is lower than the refractive index of the cladding at the periphery of the air hole can effectively reduce the BL. The introduction of 10 cores into the silica region between the 19 cores increases the lateral coupling in the core area and increases the mode field area. In this way, a large mode field dual-mode transmission with low bending loss is realized. $\Lambda = 14.5$ um, $d = 33$ um, $\Delta n = 0.0031$, $d_{center} = 4.8$ um, $\Delta n_{center} = 0.002$, $W_{trench} = 5.5$ um, $L_{trench} = 53.8$ um, and $\Delta n_1 = 0.004$ are the optimized parameters. At this time, the A_{eff} of the optical fiber HE_{11} can reach 2003.24 um^2. When the bending radius R is 1 cm, the bending loss BL is 2.57×10^{-3} dB/m. Potential applications are anticipated in the transmission of large-capacity optical communication systems and high-power lasers.

Author Contributions: Idea, conceptualization, and methodology, Y.L.; software simulation, formal analysis, investigation, resources, data curation, and writing-original draft preparation, R.J.; writing-review and editing, visualization, and supervision, Y.W.; project administration, funding acquisition, Z.L. All authors have read and agreed to the published version of the manuscript.

Institutional Review Board Statement: Not Applicable.

Informed Consent Statement: Not Applicable.

Data Availability Statement: The data in this paper are available by contacting the corresponding author (ydlian@hebut.edu.cn).

Conflicts of Interest: The authors declare no conflict of interest.

References

1. Desurvire, E.B. Capacity Demand and Technology Challenges for Lightwave Systems in the Next Two Decades. *J. Light. Technol.* **2006**, *24*, 4697–4710. [CrossRef]
2. Wang, F. Research on Equalization Technology of Mode Division Multiplexing System Based on Few Mode Fiber. Master's Thesis, University of Electronic Science and Technology of China, Chengdu, China, March 2020.
3. Cao, Y.; Shi, W.; Xu, G.; Sun, Y. Design of Bend-Resistant Large-Mode-Area Dual-Mode Photonic Crystal Fiber. *Laser Optoelectron. Prog.* **2015**, *52*, 84–90.
4. Cheo, P.K.; Liu, A.; King, G.G. A high-brightness laser beam from a phase-locked multicore Yb-doped fiber laser array. *IEEE Photonics Technol. Lett.* **2001**, *13*, 439–441. [CrossRef]
5. Zhang, Y.; Wen, W.; Yu, B.; Yuan, P. Technology of Slow Light in Photonic Crystal Waveguides. *Laser Optoelectron. Prog.* **2007**, *10*, 26–32.
6. Dai, L.; Li, T.; Jiang, C. Wideband ultralow high-order-dispersion photonic crystal slow-light waveguide. *J. OSA B* **2011**, *28*, 1622–1626. [CrossRef]
7. Baba, T. Slow light in photonic crystals. *Nat. Photonics* **2008**, *2*, 465–473. [CrossRef]
8. Saini, T.S.; Kumar, A.; Sinha, R.K. Triangular-core large-mode-area photonic crystal fiber with low bending loss for high power applications. *Appl. Opt.* **2014**, *53*, 7246–7251. [CrossRef] [PubMed]
9. Zheng, S.; Ren, G.; Lin, Z.; Jian, W.; Jian, S. Design and analysis of novel multilayer-core fiber with large mode area and low bending loss. *Opt. Commun.* **2014**, *315*, 317–323. [CrossRef]
10. Li, H.; Ren, G.; Yin, B.; Lian, Y.; Bai, Y.; Jian, W.; Jian, S. Modeling and optimized design of a parabolic-profile single-mode fiber with ultra-low bending loss and large-mode-area. *Opt. Commun.* **2015**, *352*, 84–90. [CrossRef]
11. Zheng, S.; Ren, G.; Lin, Z.; Jian, W.; Jian, S. A novel four-air-hole multicore dual-mode large-mode-area fiber: Proposal and design. *Opt. Fiber Technol.* **2013**, *19*, 419–427. [CrossRef]
12. Vogel, M.M.; Abdou-Ahmed, M.; Voss, A.; Graf, T. Very-large-mode-area, single-mode multicore fiber. *Opt. Lett.* **2009**, *34*, 2876–2878. [CrossRef]
13. Fini, J.M. Large-mode-area multicore fibers in the single-moded regime. *Opt. Express* **2011**, *19*, 4042–4046. [CrossRef]
14. Xia, C.; Bai, N.; Ozdur, I.; Zhou, X.; Li, G. Supermodes for optical transmission. *Opt. Express* **2011**, *19*, 16653–16664. [CrossRef]
15. Jin, W.; Ren, G.; Jiang, Y.; Wu, Y.; Xu, Y.; Yang, Y.; Shen, Y.; Ren, W.; Jian, S. Few-mode and large-mode-area fiber with circularly distributed cores. *Opt. Commun.* **2017**, *387*, 79–83. [CrossRef]
16. Ma, S.; Ning, T.; Lu, S.; Zheng, J.; Li, J.; Pei, L. Bending-Resistant Design of a Large Mode Area Segmented Cladding Fiber with Resonant Ring. *J. Light. Technol.* **2018**, *36*, 2844–2849. [CrossRef]
17. Wang, G.; Ning, T.; Pei, L.; Ma, S.; Zhang, J.; Zheng, J.; Li, J.; Wei, H.; Xie, C. A bending-resistant large mode area pixelated trench assisted segmented cladding fiber. *Optik* **2020**, *203*, 164024. [CrossRef]
18. Yang, M.; Lian, Y.; Wang, J.; Zhang, Y. Dual-Mode Large-Mode-Area Multicore Fiber with Air-Hole Structure. *IEEE Photonics J.* **2019**, *11*, 1–10. [CrossRef]
19. Jiang, Y.; Ren, G.; Lian, Y.; Liu, Y.; Liu, H.; Li, H.; Ren, W.; Jian, W.; Jian, S. Multilayer-core fiber with a large mode area and a low bending loss. *Chin. Opt. Lett.* **2016**, *14*, 120601. [CrossRef]
20. Ma, S.; Ning, T.; Li, J.; Zheng, J.; Wen, X.; Pei, L. Design and analysis of a modified segmented cladding fiber with large mode area. *Opt. Laser Technol.* **2017**, *88*, 172–179. [CrossRef]
21. Tong, Y.; Shuo, C.; Huiping, T. A bend-resistant low bending loss and large mode area two-layer core single-mode fiber with gradient refractive index ring and multi-trench. *Opt. Fiber Technol.* **2018**, *45*, 235–243. [CrossRef]
22. Yuqin, Z.; Yudong, L.; Yuhe, W.; Mengxin, Y.; Jingbo, W.; Nannan, L.; Yulei, W.; Zhiwei, L. Design and analysis of trench-assisted dual-mode multi-core fiber with large-mode-field-area. *Appl. Opt.* **2021**, *60*, 4698–4705.
23. Xie, X. Experimental Study of Bending Loss in Single-Mode Fiber. Master's Thesis, Beijing Jiaotong University, Beijing, China, June 2016.